

Modelling of the Aromatic Aldehyde Production by Catalytic Oxidation of Lignin in a Three-Phase Fluidized Bed Reactor

Cláudio C.B. Oliveira^{a,*}, Emerson B. Anjos^b, Jornandes D. Silva^b, Cesar A.M. Abreu^a

^aDepartment of Chemical Engineering, Federal University of Pernambuco (UFPE), Phone (81) 2126-8901, R. Prof. Artur de Sá, 50740-521, Recife - PE Brazil.

^bPolytechnic School – UPE, Laboratory of Environmental and Energetic Technology; Rua Benfca – 455, Madalena, Recife – PE, Brazil. Cep: 50750-470.

claudiothor@hotmail.com

Lignin derivatives are obtained in low levels of production by using catalytic processes in batch operations. Considering the availability of vegetable biomass with high lignin content it is processing to be economically feasible, should be conducted through continuous processes. In this way, the objective of this paper is to provide predictions for the aromatic aldehyde production from the aqueous alkaline lignin processed by wet oxidation in a three-phase fluidized bed reactor. A heterogeneous steady-state model was formulated to describe the continuous, isothermal operations of lignin oxidation associating hydrodynamic phenomena, mass transfer, and chemical reaction. The reactor operation was simulated considering a feed with 0.21 mmol/L of oxygen and 0.30 g/L of lignin at 393K and 20bar, presenting stationary profiles of the reagents and products. The mathematical model studied represented a stationary behavior and was solved by the finite difference methods in a code in FORTRAN 95.

1. Introduction

Lignocellulosic biomasses (LCB) such as energy crops and agro-industrial residues have been investigated over the last decades as sources for the sustainable production of several chemicals. LCB consists of three major components: cellulose, hemicelluloses, and lignin. These macromolecules comprise approximately 90% of the vegetable biomass. The saccharide molecules present a wide variety of functional groups, which allow the formation of compounds with different chemical structures. This feature, together with their high availability from agricultural sources, qualify them as products of increasing value as feedstocks (Oliveira et al., 2015).

The processing of extracts from organic plants has traditionally been operated in discontinuous reactors. In the case of lignocellulosic biomass, the need to conduct the manufacture of derivatives through continuous operations must appear as a mandatory option. The depolymerization of lignin through catalytic oxidation can be placed as one of the processing options, which must use the three-phase continuous reactors. In the most widespread practice of three-phase operations, in general, the mud bed reactor has been cut, whose batch production is acceptable for smaller productions. In the case of biomass, for soluble lignin, it is recommended to stagger the transformation of the mud bed to the three-phase fluidized bed.

Several chemical transformations (hydrogenolysis, oxidation, and hydrolysis) are discussed in detail in the literature for the conversion of lignin into low molar mass products (Bugg and Rahmanpour, 2015; Tsodikov et al., 2018). Lignin oxidation produces compounds of low molar mass, such as vanillin, vinyl acid, and other aromatic acids and aldehydes, used in organic syntheses (Fache et al., 2015). High molar mass lignins can be used to produce carbon fibers, polymer modifiers, adhesives, matrices for controlled release of herbicides and resins. Depending on the origin, there are differences between the lignin in the composition and the products formed by its oxidation (Tarabanko et al., 2017; Schutyser et al., 2018).

In the oxidation processes of lignin, the primary source of raw material has been lignosulphonates (Fargues et al., 1996) from the pulp and paper industry. In these cases, it is worth noting that, sometimes the objective is to obtain chemical products, sometimes is the reduction of biological oxygen demand aiming at minimizing the environmental impact when releasing lignin in the form of industrial effluents (Zhang, 2008). In both cases, the absence of catalysts requires more severe reaction conditions, thus increasing the costs of industrial installations. Thus, the study of a mathematical model will help in optimizing the process and will avoid undesirable results (Cruz and Silva, 2017; Silva and Abreu 2016).

In this sense, the objective of this paper was the development of a phenomenological mathematical model to establish and evaluate based on experimental kinetics, the operational behavior of the continuous catalytic process of wet oxidation of the alkaline lignin in a three-phase fluidized bed reactor.

2. Methodology, modelling, and simulation in a three-phase fluidized bed reactor

The modelling of three-phase catalytic processes in a gas-liquid-solid system involves a number of factors that directly and indirectly participate in the reactions, such as: gas-liquid mass transfer, gas-solid and liquid-solid, phase retention gas, dispersion of the gas phase, retention of the liquid phase, dispersion of the liquid phase, diffusive resistances in the solid, internal and external porosity (Silva, 2015).

The components present in the three-phase reactive system follow a sequence of process steps in the reactor, that is, the gaseous reagent is introduced into the gaseous phase, enters the liquid phase by mass transfer, dissolving in this and, together with the reagent of the Liquid phase, is consumed by the solid phase.

The formulation of the model was introduced by a mass balance in a differential element of reactor volume, considering that the gaseous phase is atmospheric air, and that are present in the liquid phase dissolved oxygen, lignin and oxidation reactions products.

Model equations and stationary simulation

The mass balances of the components, reagent or product, were carried out on a differential element of the fluidized bed that contain palladium catalyst supported in γ -alumina, kept in suspension in the lignin solution where it has bubbling the gas oxygen. To get the equations, a conceptual basis of the development of the axial dispersion model applied to the three-phase system involved the following considerations:

- The concurrent continuous flow of disperse phase (gas) and continuous phase;
- The theory of the two films describes the resistance to the transfer of gas-liquid and liquid-solid mass;
- The internal diffusive resistance was considered negligible, estimated through the catalyst's internal effectiveness factor, which in function of the Thiele module was practically unitary, with a view to the reduced dimensions of the particles Catalyst
- The reaction on the surface of the catalyst had its intrinsic kinetics described according to the model adopted by Sales (2001);
- The transport of mass in the axial direction was by convection and axial dispersion;
- The system was considered, without temperature gradients in the catalytic grain, as well as in the reactor;
- The steam pressure of the continuous phase was negligible compared to the pressure exerted by the oxidizing agent (atmospheric air).

Mass Balance

- The equation of the oxygen in the gas phase and liquid phase,

$$\varepsilon_j \frac{d}{dz} \left[D_{ax,j} \frac{dC_{j,O_2}(z)}{dz} \right] - \frac{4Q_j}{\pi d_c^2} \frac{dC_{j,O_2}(z)}{dz} - k_{g,l} a_{g,l} \left[\frac{C_{j,O_2}(z)}{H} - C_{j,O_2}(z) \right] = 0 \quad (1)$$

Where, "j" is the gas phase or liquid phase, ε_j is the porosity of j, $D_{ax,j}$ is the axial dispersion of j, Q_j is the flow of j, d_c is the diameter of catalyst, $k_{g,l}$ is the mass transfer constant, H is the Henry constant and C_{j,O_2} is the concentration of oxygen in j.

- The equation of the lignin in the liquid phase,

$$\varepsilon_l \frac{d}{dz} \left[D_{ax,l} \frac{dC_{l,lign}(z)}{dz} \right] - \frac{4Q_l}{\pi d_c^2} \frac{dC_{l,lign}(z)}{dz} - k_{l,s} a_{l,s} \left[C_{l,lign}(z) - C_{s,lign}(z) \right] - k_l C_l(z) C_{O_2}(z) = 0 \quad (2)$$

Where $C_{l,lign}$ is the concentration of lignin, $k_{l,s}$ is mass transfer constant, and k_l is the reaction rate constant.

- The equation of the aldehyde of the liquid phase,

$$\varepsilon_l \frac{d}{dz} \left[D_{ax,l} \frac{dC_{l,A}(z)}{dz} \right] - \frac{4Q_l}{\pi d_c^2} \frac{dC_{l,A}(z)}{dz} - k_{l,s} a_{l,s} [C_{l,A}(z) - C_{s,A}(z)] - [k_l C_{lig} C_{O_2} - k_A C_A C_{O_2}] = 0 \quad (3)$$

Where "A" is the vanillin, syringaldehyde, and p-Hydroxybenzaldehyde, and C_A is the concentration of A.

- Boundary conditions

$$D_{ax,j} \frac{dC_{j,i}(z)}{dz} \Big|_{z=0^+} = \frac{4Q_j}{\pi d_c^2} [C_{j,i}(z) \Big|_{z=0^+} - C_{j,i}(z) \Big|_{z=0^-}] \quad (4)$$

$$\frac{dC_{j,i}(z)}{dz} \Big|_{z=L} = 0 \quad (5)$$

3. Solution Methodology

To solve the proposed equations, the Finite Difference Method (DFM) was adopted. DFM is a method of solving differential equations that is based on the approximation of derivatives by finite differences. The approximation formula obtains from the Taylor series of the derivative function. The definitions below were used with the respective boundary conditions of each element, and through the method of Runge-Kutta 4th order, it was possible to obtain the profiles.

$$\frac{dC_{i,j}(z)}{dz} = \frac{1}{2\Delta z} [(C_{i,j})_{j+1} - (C_{i,j})_{j-1}] \quad (6)$$

$$\frac{dC_{i,j}(z)}{dz} = \frac{1}{\Delta z} [(C_{i,j})_j - (C_{i,j})_{j-1}] \quad (7)$$

$$\frac{d^2 C_{i,j}(z)}{dz^2} = \frac{1}{(\Delta z)^2} [(C_{i,j})_{j+1} - 2(C_{i,j})_j + (C_{i,j})_{j-1}] \quad (8)$$

$$C_{i,j}(z) = (C_{i,j})_j \quad (9)$$

4. Results and Discussion

The equations of the transformed mass balance are solved numerically with the Runge-Kutta method, implemented in Fortran PowerStation 4.0. The proposed model for this study was used to analyze the profile of chemical species throughout the reactor. Moreover, table 1 contains the parameter of entry for the simulation.

Table 1: Parameter of entry for the simulation

| Category | Symbol / Unit | Numerical Value | Category | Symbol/Unit | Numerical Value |
|-----------------------|----------------------|-----------------|-----------------------------|-------------------------------|---|
| Operating Conditions | d_c (m) | 0.05 | Gas Phase | ε_g (-) | 0.57 |
| | L (m) | 1.0 | | D_{axl} (m ² /s) | $5.316 \times 10^{-6} - 7.294 \times 10^{-6}$ |
| Initial Concentration | $C_{O_2}^0$ (mmol/L) | 0.21 | Liquid Phase | ε_L (-) | 0.49 |
| | C_{lig}^0 (mmol/L) | 0.30 | | D_{axl} (m ² /s) | $7.25 \times 10^{-6} - 9.285 \times 10^{-6}$ |
| | C_{van}^0 (mmol/L) | 0.00 | Mass Transfer Parameter | K_{gl} (m/h) | 3.77×10^{-3} |
| | C_{Sg}^0 (mmol/L) | 0.00 | | K_{is} (m/h) | 2.56×10^{-2} |
| | C_p^0 (mmol/L) | 0.00 | | a_{gl} (m ⁻¹) | 1.33×10^2 |
| | | | a_{is} (m ⁻¹) | 1.172×10^{-1} | |

As a preliminary evaluation of the domains of the operational variables' temperature and flow, operating limits were introduced for testing the simulations. In the mildest conditions of 373K and 5 L/h and higher of 393K and 10L/h, the first evaluations of the operability of the model in the stationary regime were made, simulating the oxygen and lignin profiles.

The lignin and oxygen reagents have decreasing profiles along the vertical axis of the reactor (figures 1 and 2). In the two operating flows and at the two temperatures practiced, low levels of concentration are reached, which are kept approximately 70% of the total length (0.7 z/L) of the reactor. In this way, average conversions of about 60% for lignin and 67% for oxygen are obtained, kept from the reactor medium to the exit. This aspect observed for the profiles allows indicating that the reactor can be operated with half of its height.

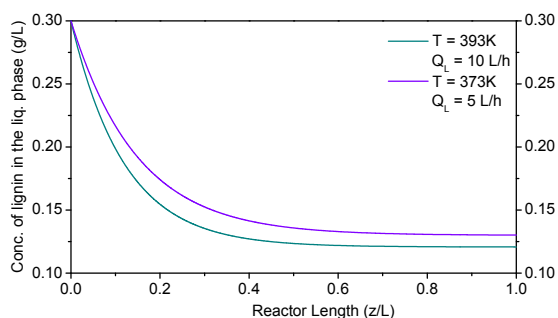


Figure 1: lignin concentration profile. Effect of liquid phase flow.

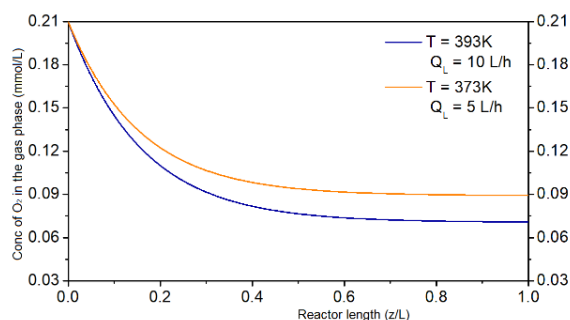


Figure 2: profile of oxygen concentration in the gas phase with the effect of flow and temperature.

The oxygen supplied by the gaseous phase supplies the liquid phase by dissolving and transferring into it (Figure 3). During the passage of the liquid phase more oxygen dissolves and is used to react with lignin and aldehydes on the catalyst, with a decrease of its concentration (0.13 mmol/L) from the reactor inlet to 70% of its length, from where it keeps constant until the exit. In the largest of the operation flows and the 393 K, more oxygen disappeared from the liquid phase, which was due to the occurrence of lower resistance to mass transfer and the most pronounced kinetic effect in contact with the catalyst.

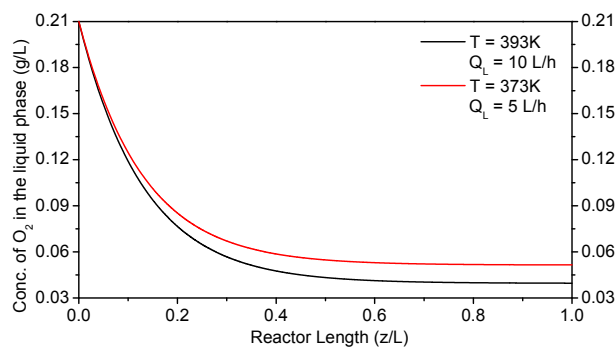


Figure 3: Oxygen concentration profile in the liquid phase. Effect of liquid phase flow and temperature.

In Figures 4 and 5, the vanillin concentration profiles were represented in the reactor, respectively in the temperatures of 373K and 393K. In each operation, the effect of the liquid phase flow operational parameter was evaluated. Validations of the model predictions are made through the profiles are formulated by simulation and compared to the experimental profiles obtained in the two flow rates of 5 L/h and 10 L/h (SALES,2001). The concentration profiles of the increasing vanillin denote that in all operations, to different flows, there is the establishment of constant levels of production of vanillin inside the reactor, at about 0.2 z/L in operation at 373K and 0.3 z/L in operation at 393K.

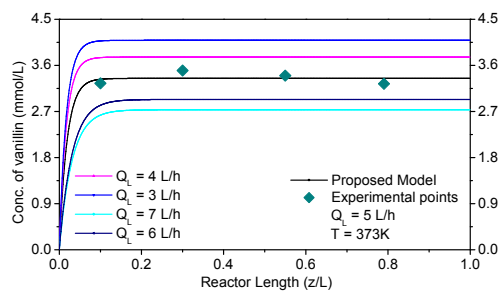


Figure 4: Vanillin concentration profile. Model validation and effect of liquid phase flow.

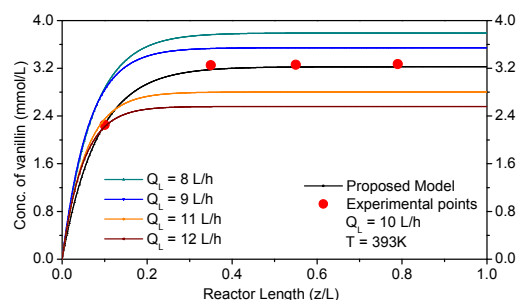


Figure 5: Vanillin concentration profile with model validation and the effect of the flow.

In Figure 6 is represented the concentration profiles of the syringaldehyde in the reactor, at the temperature of 393 K. In this operation, the effect of the liquid phase flow operational parameter was evaluated. Profile predictions are formulated by simulation and compared to the experimental profiles obtained in the flow of 5L/h and 10 L/h (Sales,2001), indicating model validation. Figure 7 represents the concentration profiles of the *p*-Hydroxybenzaldehyde in the reactor, respectively in the temperatures of 373K and 393K. In each operation, the effect of the liquid phase flow operational parameter was evaluated, reached 15 mmol/L and 13mmol/L, respectively.

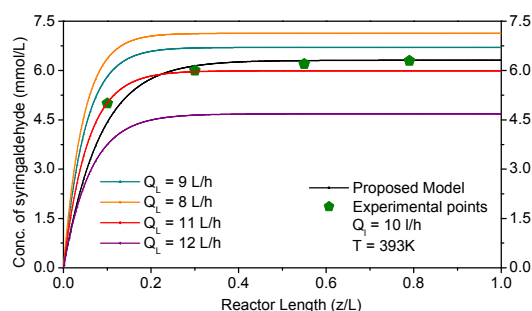


Figure 6: concentration profile of the syringaldehyde. Model validation. Effect of liquid phase flow.

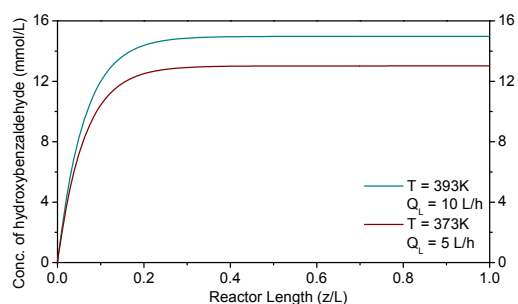


Figure 7: Concentration profile of the *p*-hydroxybenzaldehyde. Effect of liquid phase flow.

5. Conclusion

Lignocellulosic biomasses (LCB) such as energy crops and agro-industrial residues have been investigated over the last decades as sources for the sustainable production of several chemicals. In this sense, a mathematical model was developed to simulate the profile of chemical species in the oxidation processes of lignin. For this purpose, the finite difference method was used to solve the mathematical model.

- As a preliminary evaluation of the domains of the operational variables' temperature and flow, operating limits were introduced for testing the simulations. In the mildest conditions of 373K and 5 L/h and higher of 393K and 10l/h,
- The lignin and oxygen reagents have decreasing profiles along the vertical axis of the reactor
- the vanillin concentration profiles were represented in the reactor, in the temperatures of 373K and 393K. In each operation, the effect of the liquid phase flow operational parameter was evaluated. Validations of the model predictions were made through the profiles was formulated by simulation and compared to the experimental profiles obtained in the two flow rates of 5 L/h and 10 L/h (Sales,2001).
- The concentrations of the aldehydes (syringaldehyde and *p*-hydroxybenzaldehyde) increased throughout the reactor. With a higher flow rate, a more significant amount of syringaldehyde is obtained at the end of the reactor. For *p*-hydroxybenzaldehyde, the effect of the flow of the fluid phase was also observed for 10L/h and 5L/h, reaching 15 mmol/L and 13 mmol/L, respectively.

References

- Bugg, T. D., Rahmanpour, R. 2015. Enzymatic conversion of lignin into renewable chemicals. *Current opinion in chemical biology*, 29, 10-17.
- Cruz, B. M., da Silva, J. D. (2017). A two-dimensional mathematical model for the catalytic steam reforming of methane in both conventional fixed-bed and fixed-bed membrane reactors for the Production of hydrogen. *International Journal of Hydrogen Energy*, 42(37), 23670-23690.
- Fache, M., Boutevin, B., Caillol, S. 2015. Vanillin production from lignin and its use as a renewable chemical. *ACS sustainable chemistry & engineering*, 4(1), 35-46.
- Fargues, C., Mathias, Á., Rodrigues, A. 1996. Kinetics of vanillin production from kraft lignin oxidation. *Ind. engineering chemistry research*, 35(1), 28-36.
- Oliveira, C., Silva, J. D., Araujo, F. A. D., Caldas, R., Abreu, C. 2015. Kinetic Evaluation of Carbohydrate Biomass Conversions. *Chemical Engineering Transactions*, 43, 949-954.
- Sales, F.G, 2001. Catalytic wet oxidation of lignin in three-phase reactors with production of aromatic aldehyde. Campinas, SP: Doctoral thesis, State University of Campinas, graduate program in Chemical Engineering.
- Schutyser, W., Renders, T., Van den Bosch, S., Koelewijn, S. F., Beckham, G. T., Sels, B. F. 2018. Chemicals from lignin: an interplay of lignocellulose fractionation, depolymerization, and upgrading. *Chemical Society Reviews*, 47(3), 852-908.
- Silva, J. D. (2015). Numerical modelling for a catalytic trickle-bed reactor using Laplace transform technique. *Chemical Engineering Transactions*, 43, 1573-1578.
- Silva, J. D., de Abreu, C. A. M. (2016). Modelling and simulation in conventional fixed-bed and fixed-bed membrane reactors for the steam reforming of methane. *International Journal of Hydrogen Energy*, 41(27), 11660-11674.
- Tarabanko, V., Tarabanko, N. 2017. Catalytic oxidation of lignins into the aromatic aldehydes: general process trends and development prospects. *International journal of molecular sciences*, 18(11), 2421.
- Tsodikov, M., Arapova, O., Nikolaev, S. A., Chistyakov, A., Maksimov, Y. V. (2018). Benefit of Fe-containing catalytic systems for dry reforming of lignin to syngas under microwave radiation. *Chemical Engineering Transactions*, 65, 367-372.
- Zhang, Y. H. P. (2008). Reviving the carbohydrate economy via multi-product lignocellulose biorefineries. *Journal of industrial microbiology & biotechnology*, 35(5), 367-375.